10 Haptic Augmented Reality
Taxonomy, Research Status, and Challenges

Seokhee Jeon, Seungmoon Choi, and Matthias Harders

CONTENTS

10.1 INTRODUCTION

This chapter introduces an emerging research field in augmented reality (AR), called *haptic* AR. As AR enables a real space to be transformed to a semi-virtual space by providing a user with the mixed sensations of real and virtual objects, haptic AR does the same for the sense of *touch*; a user can touch a real object, a virtual object, or a real object augmented with virtual touch. Visual AR is a relatively mature technology and is being applied to diverse practical applications such as surgical training, industrial manufacturing, and entertainment (Azuma et al. 2001). In contrast, the technology

for haptic AR is quite recent and poses a great number of new research problems ranging from modeling to rendering in terms of both hardware and software.

Haptic AR promises great potential to enrich user interaction in various applications. For example, suppose that a user is holding a pen-shaped *magic* tool in the hand, which allows the user to touch and explore a virtual vase overlaid on a real table. Besides, the user may draw a picture on the table with an augmented feel of using a paint brush on a smooth piece of paper, or using a marker on a stiff white board. In a more practical setting, medical students can practice cancer palpation skills by exploring a phantom body while trying to find virtual tumors that are rendered inside the body. A consumer-targeted application can be found in online stores. Consumers can see clothes displayed on the touchscreen of a tablet computer and feel their textures with bare fingers, for which the textural and frictional properties of the touchscreen are modulated to those of the clothes. Another prominent example is augmentation or guidance of motor skills by means of external haptic (force or vibrotactile) feedback, for example, shared control or motor learning of complex skills such as driving and calligraphy. Creating such haptic modulations belongs to the realm of haptic AR. Although we have a long way to go in order to realize all the envisioned applications of haptic AR, some representative examples that have been developed in recent years are shown in Figure 10.1.

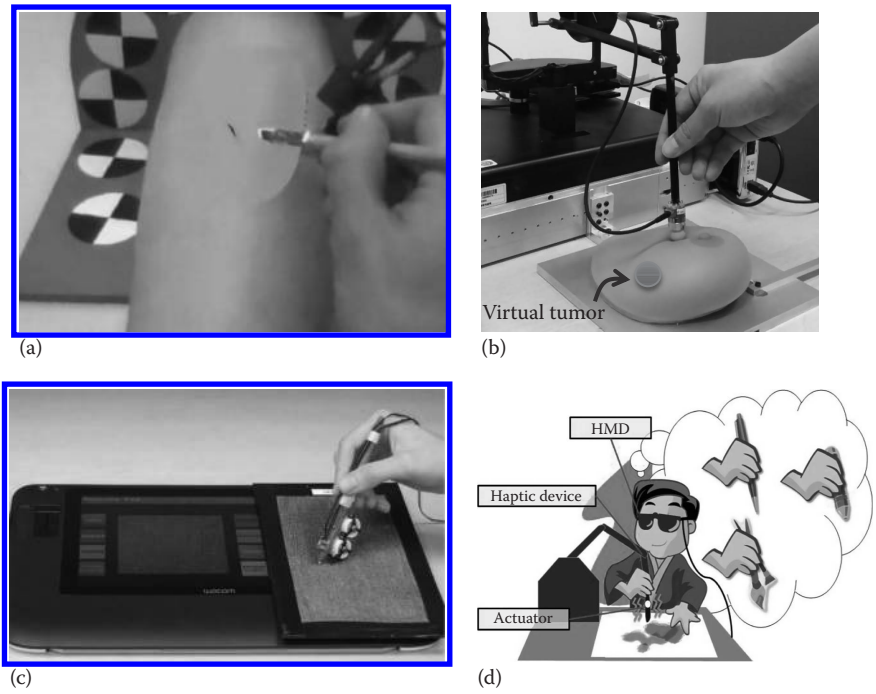

FIGURE 10.1 Representative applications of haptic AR. (a) AR-based open surgery simulator introduced. (From Harders, M. et al., *IEEE Trans. Visual. Comput. Graph.*, 15, 138, 2009.) (b) Haptic AR breast tumor palpation system. (From Jeon, S. and Harders, M., *IEEE Trans. Haptics*, 99, 1, 2014.) (c) Texture modeling and rendering based on contact acceleration data. (Reprinted from Romano, J.M. and Kuchenbecker, K.J., *IEEE Trans. Haptics*, 5, 109, 2011. With permission.) (d) Conceptual illustration of the haptic AR drawing example.

In this chapter, we first address three taxonomies for haptic AR based on a composite visuo-haptic reality–virtuality continuum, a functional aspect of haptic AR applications, and the subject of augmentation (Section 10.2). A number of studies related to haptic AR are reviewed and classified based on the three taxonomies. Based on the review, associated research issues along with components needed for a haptic AR system are elucidated in Section 10.3. Sections 10.4 through 10.6 introduce our approach for the augmentation of real object stiffness and friction, in the interaction with one or two contact points. A discussion of the open research issues for haptic AR is provided in Section 10.7, followed by brief conclusions in Section 10.8. We hope that this chapter could prompt more research interest in this exciting, yet unexplored, area of haptic AR.

10.2 TAXONOMIES

10.2.1 Visuo-Haptic Reality–Virtuality Continuum

General concepts associated with AR, or more generally, mixed reality (MR) were defined earlier by Milgram and Colquhoun Jr. (1999) using the reality–virtuality continuum shown in Figure 10.2a. The continuum includes all possible combinations of purely real and virtual environments, with the intermediate area corresponding to MR. Whether an environment is closer to reality or virtuality depends on the amount of overlay or augmentation that the computer system needs to perform; the more augmentation performed, the closer to virtuality. This criterion allows MR to be further classified into AR (e.g., a heads-up display in an aircraft cockpit) and augmented virtuality (e.g., a computer game employing a virtual dancer with the face image of a famous actress). We, however, note that the current literature does not strictly discriminate the two terms, and uses AR and MR interchangeably.

Extending the concept, we can define a similar reality–virtuality continuum for the sense of touch and construct a visuo-haptic reality–virtuality continuum by compositing the two unimodal continua shown in Figure 10.2b. This continuum can be valuable for building the taxonomy of haptic MR. In Figure 10.2b, the whole visuo-haptic continuum is classified into nine categories, and each category is named in an abbreviated form. The shaded regions belong to the realm of MR. In what follows, we review the concepts and instances associated with each category, with more attention to those of MR. Note that the continuum for touch includes all kinds of haptic feedback and does not depend on the specific types of haptic sensations (e.g., kinesthetic, tactile, or thermal) or interaction paradigms (e.g., tool-mediated or bare-handed).

In the composite continuum, the left column has the three categories of *haptic reality*, vR-hR, vMR-hR, and vV-hR, where the corresponding environments provide only real haptic sensations. Among them, the simplest category is vR-hR, which represents purely real environments without any synthetic stimuli. The other end, vV-hR, refers to the conventional visual virtual environments with real touch, for example, using a tangible prop to interact with virtual objects. Environments between the two ends belong to vMR-hR, in which a user sees mixed objects but still touches real objects. A typical example is the so-called tangible AR that has been actively studied in the visual AR community. In tangible AR, a real prop held

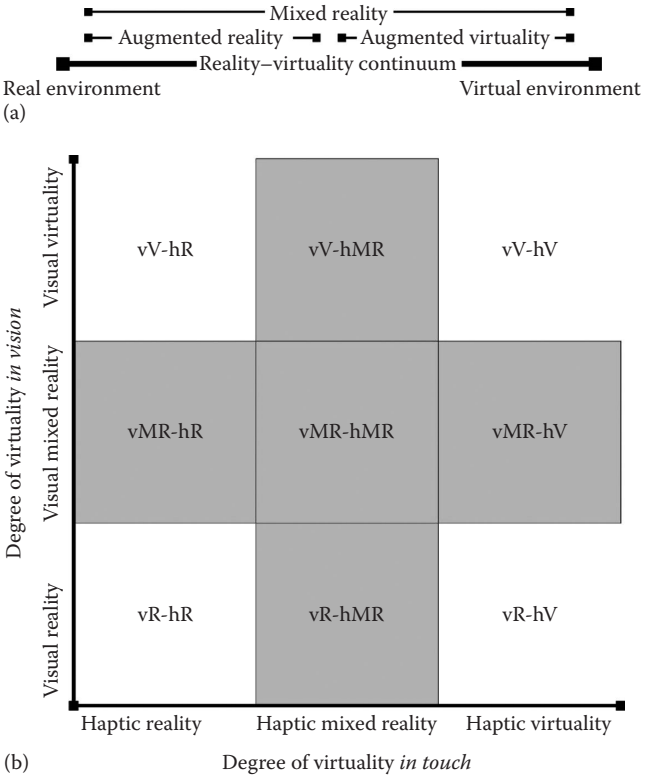

FIGURE 10.2 Reality–virtuality continuum extended to encompass touch. (Figures taken from Jeon, S. and Choi, S., *Presence Teleop. Virt. Environ*., 18, 387, 2009. With permission.) (a) Original reality–virtuality continuum. (From Milgram, P. and Colquhoun, H. Jr., A taxonomy of real and virtual world display integration, in *Mixed Reality—Merging Real and Virtual Worlds*, Y.O.A.H. Tamura (ed.), Springer-Verlag, Berlin, Germany, 1999, pp. 1–16.) (b) Composite visuo-haptic reality–virtuality continuum. (Jeon, S. and Choi, S., *Presence Teleop. Virt. Environ*., 18, 387, 2009.) Shaded areas in the composite continuum represent the realm of mixed reality.

in the hand is usually used as a tangible interface for visually mixed environments (e.g., the MagicBook in Billinghurst et al. 2001), and its haptic property is regarded unimportant for the applications. Another example is the projection augmented model. A computer-generated image is projected onto a real physical model to create a realistic-looking object, and the model can be touched by the bare hand (e.g., see Bennett and Stevens 2006). Since the material property (e.g., texture) of the real object may not agree with its visually augmented model, haptic properties are usually incorrectly displayed in this application.

The categories in the right column of the composite continuum, vR-hV, vMR-hV, and vV-hV, are for *haptic virtuality*, corresponding to environments with only virtual haptic sensations, and have received the most attention from the haptics research community. Robot-assisted motor rehabilitation can be an example of vR-hV where

synthetic haptic feedback is provided in a real visual environment, while an interactive virtual simulator is an instance of vV-hV where the sensory information of both modalities is virtual. In the intermediate category, vMR-hV, purely virtual haptic objects are placed in a visually mixed environment, and are rendered using a haptic interface on the basis of the conventional haptic rendering methods for virtual objects. Earlier attempts in this category focused on how to integrate haptic rendering of virtual objects into the existing visual AR framework, and they identified the precise registration between the haptic and the visual coordinate frame as a key issue (Adcock et al. 2003, Vallino and Brown 1999). For this topic, Kim et al. (2006) applied an adaptive low-pass filter to reduce the trembling error of a low-cost vision-based tracker using ARToolkit, and upsampled the tracking data for use with 1 kHz haptic rendering (Kim et al. 2006). Bianchi et al. further improved the registration accuracy via intensive calibration of a vision-based object tracker (Bianchi et al. 2006a,b). Their latest work explored the potential of visuo-haptic AR technology for medical training with their highly stable and accurate AR system (Harders et al. 2009). Ott et al. also applied the HMD-based visuo-haptic framework to training processes in industry and demonstrated its potential (Ott et al. 2007). In applications, a half mirror was often used for constructing a visuo-haptic framework due to the better collocation of visual and haptic feedback, for example, ImmersiveTouch (Luciano et al. 2005), Reachin Display (Reachin Technology), PARIS display (Johnson et al. 2000), and SenseGraphics 3D-IW (SenseGraphics). Such frameworks were, for instance, applied to cranial implant design (Scharver et al. 2004) or MR painting application (Sandor et al. 2007).

The last categories for *haptic MR*, vR-hMR, vMR-hMR, and vV-hMR, with which the rest of this chapter is concerned, lie in the middle column of the composite continuum. A common characteristic of haptic MR is that synthetic haptic signals that are generated by a haptic interface modulate or augment stimuli that occur due to a contact between a real object and a haptic interface medium, that is, a tool or a body part. The VisHap system (Ye et al. 2003) is an instance of vR-hMR that provides mixed haptic sensations in a real environment. In this system, some properties of a virtual object (e.g., shape and stiffness) are rendered by a haptic device, while others (e.g., texture and friction) are supplied by a real prop attached at the end-effector of the device. Other examples in this category are the SmartTool (Nojima et al. 2002) and SmartTouch systems (Kajimoto et al. 2004). They utilized various sensors (optical and electrical conductivity sensors) to capture real signals that could hardly be perceived by the bare hand, transformed the signals into haptic information, and then delivered them to the user in order to facilitate certain tasks (e.g., peeling off the white from the yolk in an egg). The MicroTactus system (Yao et al. 2004) is another example of vR-hMR, which detects and magnifies acceleration signals caused by the interaction of a pen-type probe with a real object. The system was shown to improve the performance of tissue boundary detection in arthroscopic surgical training. A similar pen-type haptic AR system, Ubi-Pen (Kyung and Lee 2009), embedded miniaturized texture and vibrotactile displays in the pen, adding realistic tactile feedback for interaction with a touch screen in mobile devices.

On the other hand, environments in vV-hMR use synthetic visual stimuli. For example, Borst et al. investigated the utility of haptic MR in a visual virtual environment

by adding synthetic force to a passive haptic response for a panel control task (Borst and Volz 2005). Their results showed that mixed force feedback was better than synthetic force alone in terms of task performance and user preference. In vMR-hMR, both modalities rely on mixed stimuli. Ha et al. installed a vibrator in a real tangible prop to produce virtual vibrotactile sensations in addition to the real haptic information of the prop in a visually mixed environment (Ha et al. 2007). They demonstrated that the virtual vibrotactile feedback enhances immersion for an AR-based handheld game. Bayart et al. introduced a teleoperation framework where force measured at the remote site is presented at the master side with additional virtual force and mixed imagery (Bayart et al. 2007, 2008). In particular, they tried to modulate a certain real haptic property with virtual force feedback for a hole-patching task and a painting application, unlike most of the related studies introduced earlier.

Several remarks need to be made. First, the vast majority of related work, except (Bayart et al. 2008, Borst and Volz 2005, Nojima et al. 2002), has used the term *haptic AR* without distinguishing vMR-hV and hMR, although research issues associated with the two categories are fundamentally different. Second, haptic MR can be further classified to *haptic AR* and *haptic augmented virtuality* using the same criterion of visual MR. All of the research instances of hMR introduced earlier correspond to haptic AR, since little knowledge regarding an environment is managed by the computer for haptic augmentation. However, despite its potential, attempts to develop systematic and general computational algorithms for haptic AR have been scanty. An instance of haptic augmented virtuality can be haptic rendering systems that use haptic signals captured from a real object (e.g., see Hoever et al. 2009, Okamura et al. 2001, Pai et al. 2001, Romano and Kuchenbecker 2011) in addition to virtual object rendering, although such a concept has not been formalized before. Third, although the taxonomy is defined for composite visuo-haptic configurations, a unimodal case (e.g., no haptic or visual feedback) can also be mapped to the corresponding 1D continuum on the axes in Figure 10.2b.

10.2.2 Artificial Recreation and Augmented Perception

The taxonomy described in the previous section is based on the visuo-haptic reality–virtuality continuum, thereby elucidating the nature of stimuli provided to users and associated research issues. Also useful is a taxonomy that specifies the *aims* of augmentation. Hugues et al. (2011) defined two functional categories for visual AR: *artificial recreation (or environment)* and *augmented perception*, which can be also applied to hMR category in Figure 10.2. This is in line with the terms used by Bayart and Kheddar (2006)—haptic enhancing and enhanced haptics, respectively.

In artificial recreation, haptic augmentation is used to provide a realistic presentation of physical entities by exploiting the crucial advantage of AR, that is, more efficient and realistic construction of an immersive environment, compared to VR. Artificial recreation can be further classified into two sub-categories. It can be either for realistic reproduction of a specific physical environment, for example, the texture display example of clothes described in Section 10.1, or for creating a nonexisting environment, for example, the tumor palpation example in Jeon et al. (2012). The latter is a particularly important area for haptic AR, since it maximizes the advantages of both VR and AR.

In contrast, augmented perception aims at utilizing touch as an additional channel for transferring useful information that can assist decision-making. Since realism is no longer a concern, the form of virtual haptic stimuli in this category significantly varies depending on the target usage. For example, one of the simplest forms is vibration alerts. Synthetic vibratory signals, while mixed with other haptic attributes of the environment, are a powerful means of conveying timing information, for example, mobile phone alarms, driving hazard warnings (Chun et al. 2013), and rhythmic guidance (Lee et al. 2012b). Recently, many researchers also tried to use vibration for spatial information (e.g., Lee and Choi 2014, Sreng et al. 2008) and discrete categorical information (e.g., haptic icon [Rovers and van Essen 2004, Ternes and MacLean 2008]).

Force feedback is another widely used form for augmentation in this category. The most common example is virtual fixtures used for haptic guidance. They add guiding or preventing forces to the operator's movement while she/he performs a motor task, in order to improve the safety, accuracy, and speed of task execution (Abbott et al. 2007). The term was originally coined in Rosenberg (1993), and it has been applied to various areas, for example, a manual milling tool (Zoran and Paradiso 2012), the SmartTool (Nojima et al. 2002), or surgical assistance systems (Li et al. 2007).

There have also been attempts that faithfully follow the original meaning of *augmentation of reality*. The aforementioned MicroTactus system (Yao et al. 2004) is one example. Sometimes, augmentation is done by mapping nonhaptic information into haptic cues for the purpose of data perceptualization, for example, color information mapped to tactile stimuli (Kajimoto et al. 2004). Another interesting concept is diminished reality, which hides reality, for example, removing the surface haptic texture of a physical object (Ochiai et al. 2014). This concept of diminished reality can also be applied to hand tremor cancellation in surgical operations (Gopal et al. 2013, Mitchell et al. 2007). Lastly, in a broad sense, exoskeletal suits are also an example of augmentation through mixing real and virtual force.

10.2.3 Within- and Between-Property Augmentation

Various physical properties, such as shape, stiffness, friction, viscosity, and surface texture, contribute to haptic perception. Depending on the haptic AR scenario, some object properties may remain intact while the rest may be subject to augmentation. Here, the augmentation may occur *within* a property, for example, mixing real and virtual stiffness for rendering harder virtual nodules inside a tissue phantom (Jeon et al. 2012), or it may be *between* different properties, for example, adding virtual stiffness to real surface textures (Yokokohji et al. 1999) or vice versa (Borst and Volz 2005).

This distinction is particularly useful for gauging the degree, accuracy, and type of registration needed for augmentation. Consequently, this taxonomy allows the developer to quantify the amount of environment modeling necessary for registration in preprocessing and rendering steps. The next section further describes issues and requirements for registration and environment modeling for haptic AR.

TABLE 10.1
Classification of Related Studies Using the Composite Taxonomy

	Artificial Recreation	Augmented Perception
Within-property augmentation	Borst and Volz (2005)	Abbott and Okamura (2003)
	Jeon and Choi (2009)	Bose et al. (1992)
	Jeon and Choi (2011)	Gopal et al. (2013)
	Jeon et al. (2012)	Kajimoto et al. (2004)
	Jeon et al. (2011)	Mitchell et al. (2007)
	Jeon and Harders (2014)	Nojima et al. (2002)
	SoIanki and Raja (2010)	Ochiai et al. (2014)
	Gerling and Thomas (2005)	Yao et al. (2004)
	Kurita et al. (2009)	Yang et al. (2008)
	Hachisu et al. (2012)	Lee et al. (2012a)
Between-property augmentation	Bayart et al. (2008)	Brewster and Brown (2004)
	Bayart et al. (2007)	Brown and Kaaresoja (2006)
	Fukumoto and Sugimura (2001)	Kim and Kim (2012)
	Iwata et al. (2001)	Kyung and Lee (2009)
	Minamizawa et al. (2007)	Lee and Choi (2014)
	Park et al. (2011)	Powell and O'Malley (2011)
	Ye et al. (2003)	Rosenberg (1993)
	Yokokohji et al. (1999)	Spence and Ho (2008)
	Frey et al. (2006)	Zoran and Paradiso (2012)
	Parkes et al. (2009)	Grosshauser and Hermann (2009)
	Ha et al. (2006)	
	Romano and Kuchenbecker (2011)	

Further, the last two taxonomies are combined to construct a composite taxonomy, and all relevant literature in the hMR category is classified using this taxonomy in Table 10.1. Note that most of the haptic AR systems have both within- and between-property characteristics to some degree. For clear classification, we only examined key augmentation features in Table 10.1.

10.3 COMPONENTS REQUIRED FOR HAPTIC AR

10.3.1 Interface for Haptic AR

A haptic AR framework inherently involves interactions with real environments. Therefore, three systems—a haptic interface, a human operator, and a real environment—react to each other through an *interaction tool*, leading to tridirectional interaction as shown in Figure 10.3.

During interaction, the interaction tool is coupled with the three components, and this coupling is the core for the realization of haptic AR, that is, merging the real and the virtual. Through this coupled tool, relevant physical signals from

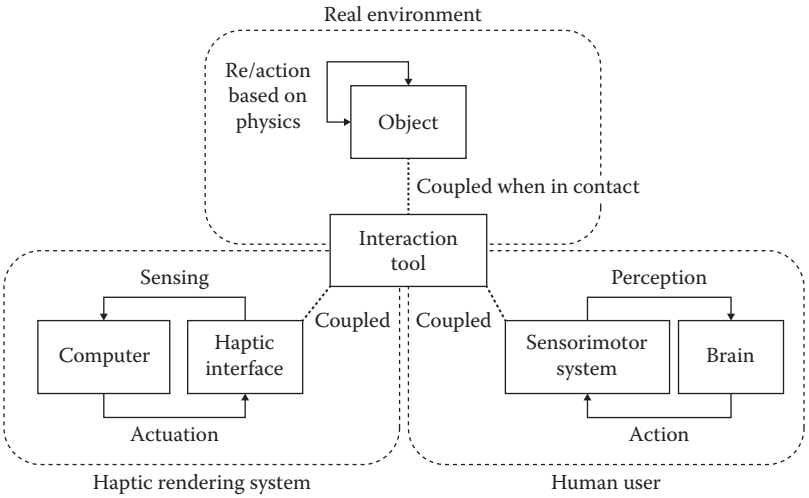

FIGURE 10.3 Tridirectional interaction in haptic AR.

both the real environment and the haptic interface are mixed and transmitted to the user. Therefore, designing this *feel-through* tool is of substantial importance in designing a haptic AR interface.

The feel-through can be either direct or indirect. Direct feel-through, analogous to optical see-through in visual AR, transmits relevant physical signals directly to the user via a mechanically coupled implement. In contrast, in indirect feel-through (similar to video see-through), relevant physical signals are sensed, modeled, and synthetically reconstructed for the user to feel, for example, in master–slave teleoperation. In direct feel-through, preserving the realism of a real environment and mixing real and virtual stimuli is relatively easy, but real signals must be compensated for with great care for augmentation. To this end, the system may need to employ very accurate real response estimation methods for active compensation or special hardware for passive compensation, for example, using a ball bearing tip to remove friction (Jeon and Choi 2010) and using a deformable tip to compensate for real contact vibration (Hachisu et al. 2012). On the contrary, in indirect feel-through, modulating real signals is easier since all the final stimuli are synthesized, but more sophisticated hardware is required for transparent rendering of virtual stimuli with high realism.

Different kinds of coupling may exist. Mechanical coupling is a typical example, a force feedback haptic stylus instrumented with a contact tip, for example (Jeon and Choi 2011). Other forms such as *thermal* coupling and *electric* coupling are also possible depending on the target property. In between-property augmentation, coupling may not be very tight, for example, only position data and timing are shared (Borst and Volz 2005).

Haptic AR tools can come in many different forms. In addition to typical styli, very thin sheath-type tools are also used, for example, sensors on one side and

actuators on the other side of a sheath (Nojima et al. 2002). Sometimes a real object itself is a tool, for example, when both sensing and actuation modules are embedded in a tangible marker (Ha et al. 2006).

A tool and coupling for haptic AR needs to be very carefully designed. Each of the three components involved in the interaction requires a proper attachment to the tool, appropriate sensing and actuation capability, and eventually, all of these should be compactly integrated into the tool in a way that it can be appropriately used by a user. To this end, the form factors of the sensors, attachment joints, and actuation parts should be carefully designed to maximize the reliability of sensing and actuation while maintaining a sufficient degree of freedom of movement.

10.3.2 Registration between Real and Virtual Stimuli

An AR system generally faces two registration problems between real and virtual environments: spatial and temporal registrations. Virtual and real stimuli must be spatially and temporally aligned with each other with high accuracy and robustness. In visual AR, proper alignment of virtual graphics (usually in 3D) on real video streams has been a major research issue (Feng et al. 2008). Tracking an AR camera, a user, and real objects and localizing them in a world coordinate frame are the core technical problems (Harders et al. 2009).

In haptic AR, virtual and real haptic stimuli also have to be spatially and temporally aligned, for example, adding a virtual force at the right position and at the right moment. While sharing the same principle, registration in haptic AR sometimes has different technical requirements. In many haptic AR scenarios, an area of interest for touching is very small (even one or a couple of points), and touch usually occurs via a tool. Therefore, large area tracking used in visual AR is not necessary, and tracking can be simplified, for example, detecting the moment and location of contact between a haptic tool and a real object using a mechanical tracker. However, tracking data are directly used for haptic rendering in many cases, so the update rate and accuracy of tracking should be carefully considered.

In addition to such basic position and timing registration, other forms of spatial and temporal quantities related to the target augmentation property often require adequate alignment. For example, in order to augment stiffness, the direction of force for virtual stiffness must be aligned with the response force direction from real stiffness. Another example is an AR pulse simulator where the frequency and phase of a virtual heart beat should match with those of the real one. These alignments usually can be done by acquiring the real quantity through sophisticated real-time sensing and/or estimation modules and setting corresponding virtual values to them. Examining and designing such property-related registration is one of the major research issues in developing haptic AR systems.

The requirements of this property-related registration largely depend on an application area, a target augmentation property, and physical signals involved. However, the within/between-property taxonomy can provide some clues for judging what kinds of and how accurate registration is needed, as the taxonomy gives the degree of association

between virtual and real signals. In the case of within-property augmentation, mixing happens in a single property, and thus virtual signals related to a target property need to be exactly aligned with corresponding real signals for harmonious merging and smooth transition along the line between real and virtual. This needs very sophisticated registration, often with the estimation of real properties based on sensors and environment models (see Section 10.4 for how we have approached this issue). However, in between-property augmentation, different properties are usually treated separately, and virtual signals of one target property do not have to be closely associated with real signals of the other properties. Thus, the registration may be of lesser accuracy in this case.

10.3.3 Rendering Algorithm for Augmentation

A rendering frame of an AR system consists of (1) sensing the real environment, (2) real–virtual registration, (3) merging stimuli, and (4) displaying the stimuli. The following paragraphs overview the steps for haptic AR. Steps 2 and 3 are the core parts for haptic AR.

Step 1 prepares data for steps 2 and 3 by sensing variables from the real environment. Signal processing can also be applied to the sensor values.

Step 2 conducts a registration process based on the sensed data and pre-identified models (see Section 10.3.4 for examples). This step usually estimates the spatial and temporal state of the tool and the real environment and then conducts the registration as indicated in Section 10.3.2, for example, property-related registration and contact detection between the tool and real objects. Depending on the result of this step, the system decides whether to proceed to step 3 or go back to step 1 in this frame.

Step 3 is dedicated to the actual calculation of virtual feedback (in direct feel-through) or mixed feedback (in indirect feel-through). Computational procedures in this step largely depend on the categories of haptic AR (Table 10.1). For artificial recreation, this step simulates the behaviors of the properties involved in the rendering using physically based models. However, augmented perception may need to derive the target signal based on purely sensed signals and/or using simpler rules, for example, doubling the amplitude of measured contact vibration (Yao et al. 2004). In addition, within-property augmentation often requires an estimation of the properties of a real object in order to compensate for or augment it. For instance, modulating the feel of a brush in the AR drawing example first needs the compensation of the real tension and friction of the manipulandum. This estimation can be done either using a model already identified in a preprocessing step or by real-time estimation of the property using sensor values, or both (see Section 10.3.4 for more details). In between-property augmentation, however, this estimation process is not required in general, and providing virtual properties is simpler.

Step 4 sends commands to the haptic AR interface to display the feedback calculated in Step 3. Sometimes we need techniques for controlling the hardware for the precise delivery of stimuli.

10.3.4 Models for Haptic AR

As aforementioned in Sections 10.3.2 and 10.3.3, haptic AR requires predefined models for three different purposes. First, models are needed for simulating the responses of the signals associated with rendering properties, which is the same for haptic VR rendering. Such computational models have been extensively studied in haptics and virtual reality. In most cases, they include some degree of simplification to fulfill the real-time requirement of haptic rendering.

The second model is for real–virtual registration (Step 2 in Section 10.3.3). The most common example is the geometry model of real objects for contact and surface normal detection, which is usually built in preprocessing. Employing such a geometry model makes rendering simpler since conventional rendering algorithms for haptic VR can be readily applied. However, acquiring and using such models should be minimized in order to fully utilize the general advantage of AR: efficient construction of a realistic and immersive environment without extensive modeling. Balancing the amount of modeling and complexity of rendering algorithm is important. In addition to geometry models, property augmentation sometimes needs models for the estimation of real information. For example, in Section 10.4, we estimate local geometry and local deformation near to the contact point based on a simplified environment model that is identified in preprocessing in order for stiffness direction registration.

The last model is for the estimation of real signals in order for modulation in Step 3 of the rendering (Section 10.3.3). The estimation often has challenging accuracy requirements while still preserving efficiency for real-time performance. For properties such as stiffness and friction, estimating physical responses has been extensively studied in robotics and mechatronics for the purpose of environment modeling and/or compensation. In general, there are two approaches for this: open-loop model-based estimation and closed-loop sensor-based estimation. One of the research issues is how to adapt those techniques for use in haptic AR, which has the following requirements. The estimation should be perceptually accurate since the errors in estimation can be directly fed into the final stimuli. The identification process should also be feasible for the application, for example, very quick identification is mandatory for scenarios in which real objects for interaction frequently change. Lastly, using the same hardware for both identification and rendering is preferred for the usability of the system.

Each category in Table 10.1 has different requirements for models. Systems in the artificial recreation category may need more sophisticated models for both simulation and estimation, while those in the augmenting perception category may suffice with simpler model for simulation. Furthermore, systems in the between-property category may have to use very accurate registration and estimation models, while merging between properties may not need models for registration and estimation.

For summary, Table 10.2 outlines the rendering and registration characteristics of the categories in the two taxonomies.

In the following sections, we introduce example algorithms for haptic AR, targeting a system that can modulate stiffness and friction of a real object by systematically adding virtual stiffness and friction.

TABLE 10.2
Characteristics of the Categories

Category	Within Property	Between Property
Registration and rendering	• Registration: position and timing registration as well as property-related registration needed. • Rendering includes estimation and compensation of real signals and merging of them with virtual signals.	• Registration: only basic position and timing registration needed. • Rendering: algorithms for haptic VR can be applied.
Category	**Artificial Recreation**	**Augmented Perception**
Models required	• Models for physics simulation. • Sometimes models for registration and compensation.	• Models for registration and compensation.
Category	**Direct Feel-Through**	**Indirect Feel-Through**
Rendering	• Real-time compensation of real property needed.	• Transparent haptic rendering algorithm and interface needed.

10.4 STIFFNESS MODULATION

We initiated our endeavor toward haptic AR with the augmentation or modulation of real object stiffness, which is one of the most important properties for rendering the shape and hardness of an object. We summarize a series of our major results on stiffness modulation (Jeon and Choi 2008, 2009, 2010, 2011; Jeon and Harders 2012) in the following sections. This topic can be categorized into artificial recreation and within-property augmentation.

We aim at providing a user with augmented stiffness by adding virtual force feedback when interacting with real objects. We took two steps for this goal. The first step was single-point interaction supporting typical exploratory patterns, such as tapping, stroking, or contour following (Section 10.4.2). The second step extended the first system to two-point manipulation, focusing on grasping and squeezing (Section 10.4.3).

Our augmentation methods emphasize minimizing the need for prior knowledge and preprocessing, for example, the geometric model of a real object, used for registration, while preserving plausible perceptual quality. Our system requires a minimal amount of prior information such as the dynamics model of a real object. This preserves a crucial advantage of AR; only models for the objects of interest, not the entire environment, are required, which potentially leads to greater simplicity in application development.

Our framework considers elastic objects with moderate stiffness for interaction. Objects made of plastic (e.g., clay), brittle (e.g., glass), or high stiffness material (e.g., steel) are out of scope due to either complex material behavior or the performance limitations of current haptic devices. In addition, homogeneous dynamic material responses are assumed for real objects.

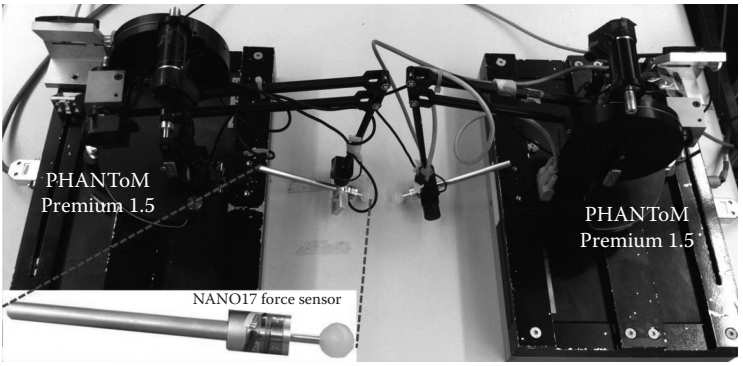

FIGURE 10.4 Haptic AR interface. (Reprinted from Jeon, S. and Harders, M., Extending haptic augmented reality: Modulating stiffness during two-point squeezing, in *Proceedings of the Haptics Symposium*, 2012, pp. 141–146. With permission.)

10.4.1 Haptic AR Interface

We constructed a haptic AR interface using two general impedance-type haptic interfaces (Geomagic; PHANToM premium model 1.5), each of which has a custom-designed tool for interaction with a real object (see Figure 10.4). The tool is instrumented with a 3D force/torque sensor (ATI Industrial Automation, Inc.; model Nano17) attached between the tool tip and the gimbal joints at the last link of the PHANToM. This allows the system to measure the reaction force from a real object that is equal to the sum of the force from the haptic interface and the force from the user's hand.

10.4.2 Stiffness Modulation in Single-Contact Interaction

Suppose that a user indents a real object with a probing tool. This makes the object deform, and the user feels a reaction force. Let the apparent stiffness of the object at time t be $k(t)$. This is the stiffness that the user perceives when no additional virtual force is rendered. The goal of stiffness augmentation is to systematically change the stiffness that the user perceives $k(t)$ to a desired stiffness $\tilde{k}(t)$ by providing virtual force to the user.

As shown in Figure 10.5, two force components, the force that the haptic device exerts to the tool, $\mathbf{f}_d(t)$, and the force from the user's hand, $\mathbf{f}_h(t)$, deform the object surface and result in a reaction force $\mathbf{f}_r(t)$, such that

$$\mathbf{f}_r(t) = -\left\{\mathbf{f}_h(t) + \mathbf{f}_d(t)\right\}. \tag{10.1}$$

The reaction force $\mathbf{f}_r(t)$ during contact can be decomposed into two orthogonal force components, as shown in Figure 10.5:

$$\mathbf{f}_r(t) = \mathbf{f}_r^n(t) + \mathbf{f}_r^t(t), \tag{10.2}$$

where

$\mathbf{f}_r^n(t)$ is the result of object elasticity in the normal direction
$\mathbf{f}_r^t(t)$ is the frictional tangential force

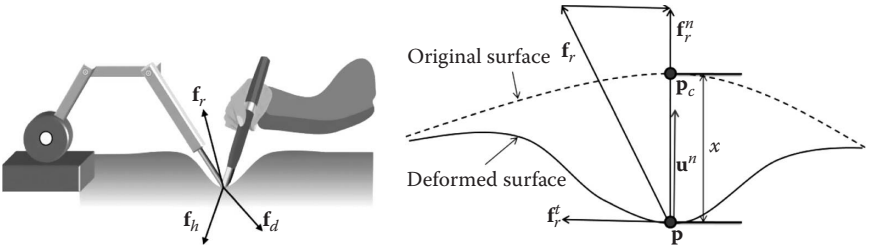

FIGURE 10.5 Variables for single-contact stiffness modulation. (Reprinted from Jeon, S. and Choi, S., *Presence Teleop. Virt. Environ*., 20, 337, 2011. With permission.)

Let $x(t)$ be the displacement caused by the elastic force component, which represents the distance between the haptic interface tool position, $\mathbf{p}(t)$, and the original non-deformed position $\mathbf{p}_c(t)$ of a contacted particle on the object surface. If we denote the unit vector in the direction of $\mathbf{f}_r^n(t)$ by $\mathbf{u}^n(t)$ and the target modulation stiffness by $\tilde{k}(t)$, the force that a user should feel is:

$$\tilde{\mathbf{f}}_h(t) = \tilde{k}(t)\, x(t)\mathbf{u}^n(t). \tag{10.3}$$

Using (10.3), the force that the haptic device needs to exert is

$$\tilde{\mathbf{f}}_d(t) = -\mathbf{f}_r(t) - \tilde{k}(t)\, x(t)\mathbf{u}^n(t). \tag{10.4}$$

This equation indicates the tasks that a stiffness modulation algorithm has to do in every loop: (1) detection of the contact between the haptic tool and the real object for spatial and temporal registration, (2) measurement of the reaction force $\mathbf{f}_r(t)$, (3) estimation of the direction $\mathbf{u}^n(t)$ and magnitude $x(t)$ of the resulting deformation for stiffness augmentation, and (4) control of the device-rendered force $\mathbf{f}_d(t)$ to produce the desired force $\tilde{\mathbf{f}}_d(t)$. The following section describes how we address these four steps.

In Step 1, we use force sensor readings for contact detection since the entire geometry of the real environment is not available. A collision is regarded to have occurred when forces sensed during interaction exceed a threshold. To increase the accuracy, we developed algorithms to suppress noise, as well as to compensate for the weight and dynamic effects of the tool. See Jeon and Choi (2011) for details. Step 2 is also simply done with the force sensor attached to the probing tool.

Step 3 is the key process for stiffness modulation. We first identify the friction and deformation dynamics of a real object in a preprocessing step, and use them later during rendering to estimate the known variables for merging real and virtual forces. The details of this process are summarized in the following section.

Before augmentation, we carry out two preprocessing steps. First, the friction between the real object and the tool tip is identified using the Dahl friction model (Jeon and Choi 2011). The original Dahl model is transformed to an equivalent discrete-time difference equation, as described in Mahvash and Okamura (2006). It also includes a velocity-dependent term to cope with viscous friction. The procedure for friction

identification adapts the divide-and-conquer strategy by performing identification separately for the presliding and the sliding regime, which decouples the nonlinear identification problem to two linear problems. Data for lateral displacement, velocity, normal force, and friction force are collected during manual stroking, and then are divided into presliding and sliding bins according to the lateral displacement. The data bins for the presliding regime are used to identify the parameters that define behavior at almost zero velocity, while the others are used for Coulomb and viscous parameters.

The second preprocessing step is for identifying the deformation dynamics of the real object. We use the Hunt–Crossley model (Hunt and Crossley 1975) to account for nonlinearity. The model determines the response force magnitude given displacement $x(t)$ and velocity $\dot{x}(t)$ by

$$f(t) = k\left(x(t)\right)^m + b\left(x(t)\right)^m \dot{x}(t), \tag{10.5}$$

where

k and b are stiffness and damping constants
m is a constant exponent (usually $1 < m < 2$)

For identification, the data triples consisting of displacement, velocity, and reaction force magnitude are collected through repeated presses and releases of a deformable sample in the normal direction. The data are passed to a recursive least-squares algorithm for an iterative estimation of the Hunt–Crossley model parameters (Haddadi and Hashtrudi-Zaad 2008).

For rendering, the following computational process is executed in every haptic rendering frame. First, two variables, the deformation direction $\mathbf{u}^n(t)$ and the magnitude of the deformation $x(t)$ are estimated. The former is derived as follows. Equation 10.2 indicates that the response force $\mathbf{f}_r(t)$ consists of two perpendicular force components: $\mathbf{f}_r^n(t)$ and $\mathbf{f}_r^t(t)$. Since $\mathbf{u}^n(t)$ is the unit vector of $\mathbf{f}_r^n(t)$, $\mathbf{u}^n(t)$ becomes:

$$\mathbf{u}^n(t) = \frac{\mathbf{f}_r(t) - \mathbf{f}_r^t(t)}{\left|\mathbf{f}_r(t) - \mathbf{f}_r^t(t)\right|}. \tag{10.6}$$

The known variable in (10.6) is $\mathbf{f}_r^t(t)$. The magnitude of $\mathbf{f}_r^t(t)$ is estimated using the identified Dahl model. Its direction is derived from the tangent vector at the current contact point $\mathbf{p}(t)$, which is found by projecting $\Delta\mathbf{p}(t)$ onto $\mathbf{u}^n(t-\Delta t)$ and subtracting it from $\Delta\mathbf{p}(t)$.

The next part is the estimation of $x(t)$. The assumption of material homogeneity allows us to directly approximate it from the inverse of the Hunt–Crossley model identified previously. Finally, using the estimated $\mathbf{u}^n(t)$ and $x(t)$, $\tilde{\mathbf{f}}_d(t)$ is calculated using (10.4), which is then sent to the haptic AR interface.

In Jeon and Choi (2011), we assessed the physical performance of each component and the perceptual performance of the final rendering result using various real samples. In particular, the perceptual quality of modulated stiffness evaluated in a

psychophysical experiment showed that rendering errors were less than the human discriminability of stiffness. This demonstrates that our system can provide perceptually convincing stiffness modulation.

10.4.3 Stiffness Modulation in Two-Contact Squeezing

After confirming the potential of the concept, we moved to a more challenging scenario: stiffness modulation in two-contact squeezing (Jeon and Harders 2012). We developed new algorithms to provide stiffness augmentation while grasping and squeezing an object with two probing tools. In this system, we assume that the object is fully lifted from the ground and the contact points do not change without slip. We also do not take inertial effects into account.

During lifting an object, an additional force due to the object weight, $\mathbf{f}_w(t)$ in Figure 10.6, is involved in the system. When the user applies forces $\mathbf{f}_{h,*}(t)$ to hold and squeeze the object (* is either 1 or 2 depending on the contact point) and the haptic interfaces exert forces $\mathbf{f}_{d,*}(t)$ for modulation, weight forces $\mathbf{f}_{w,*}(t)$ are also present at the two contact points. At each contact point, these three force components deform the object and make reaction force $\mathbf{f}_{r,*}(t)$:

$$\mathbf{f}_{r,*}(t) = \mathbf{f}_{h,*}(t) + \mathbf{f}_{d,*}(t) + \mathbf{f}_{w,*}(t). \tag{10.7}$$

$\mathbf{f}_{r,*}(t)$ can be further decomposed to pure weight $\mathbf{f}_{w,*}(t)$ and a force component in squeezing direction $\mathbf{f}_{sqz,*}(t)$ as shown in Figure 10.6, resulting in

$$\mathbf{f}_{r,*}(t) = \mathbf{f}_{sqz,*}(t) + \mathbf{f}_{w,*}(t). \tag{10.8}$$

Since the displacement and the force along the squeezing direction contribute to stiffness perception, the force component of interest is $\mathbf{f}_{sqz,*}(t)$. Then, (10.7) can be rewritten as

$$\mathbf{f}_{sqz,*}(t) = \mathbf{f}_{h,*}(t) + \mathbf{f}_{d,*}(t). \tag{10.9}$$

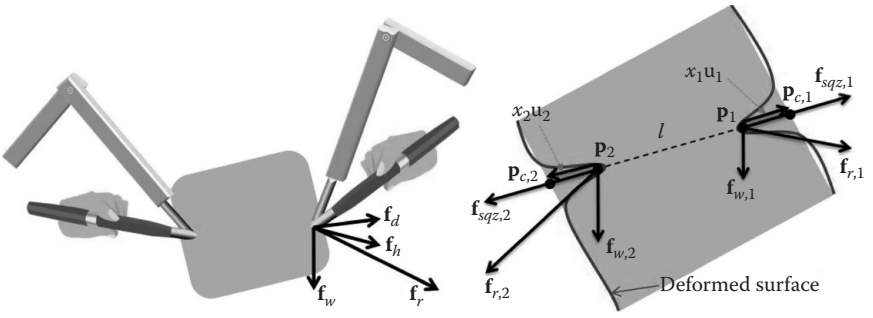

FIGURE 10.6 Variables for two-contact stiffness modulation. (Reprinted from Jeon, S. and Harders, M., Extending haptic augmented reality: Modulating stiffness during two-point squeezing, in *Proceedings of the Haptics Symposium*, 2012, pp. 141–146. With permission.)

To make the user feel the desired stiffness $\tilde{k}(t)$,

$$\mathbf{f}_{h,*}(t) = \tilde{k}(t)\, x_*(t)\, \mathbf{u}_*(t), \tag{10.10}$$

where $x_*(t)$ represents the displacement along the squeezing direction and $\mathbf{u}_*(t)$ is the unit vector toward the direction of that deformation. Combining (10.9) and (10.10) results in the virtual force for the haptic interfaces to render for the desired augmentation:

$$\tilde{\mathbf{f}}_{d,*}(t) = \mathbf{f}_{sqz,*}(t) - \tilde{k}(t)\, x_*(t)\, \mathbf{u}_*(t). \tag{10.11}$$

Here again, (10.11) indicates that we need to estimate the displacement $x_*(t)$ and the deformation direction $\mathbf{u}_*(t)$ at each contact point. The known variables are the reaction forces $\mathbf{f}_{r,*}(t)$ and the tool tip positions $\mathbf{p}_*(t)$. To this end, the following three observations about an object held in the steady state are utilized. First, the magnitudes of the two squeezing forces $\mathbf{f}_{sqz,1}(t)$ and $\mathbf{f}_{sqz,2}(t)$ are the same, but the directions are the opposite ($\mathbf{f}_{sqz,1}(t) = -\mathbf{f}_{sqz,2}(t)$). Second, each squeezing force falls on the line connecting the two contact locations. Third, the total weight of the object is equal to the sum of the two reaction force vectors:

$$\mathbf{f}_{r,1}(t) + \mathbf{f}_{r,2}(t) = \mathbf{f}_{w,1}(t) + \mathbf{f}_{w,2}(t).$$

The first and second observations provide the directions of $\mathbf{f}_{sqz,*}(t)$ (= $\mathbf{u}_*(t)$ = $\overrightarrow{\mathbf{p}_1(t)\mathbf{p}_2(t)}$ or $\overrightarrow{\mathbf{p}_2(t)\mathbf{p}_1(t)}$; also see $l(t)$ in Figure 10.6). The magnitude of $\mathbf{f}_{sqz,*}(t)$, $f_{sqz,*}(t)$ is determined as follows. The sum of the reaction forces along the $l(t)$ direction, $f_{r_{\downarrow}sqz}(t) = \left|\mathbf{f}_{r,1}(t)\cdot\mathbf{u}_l(t)\right| + \left|\mathbf{f}_{r,2}(t)\cdot\mathbf{u}_l(t)\right|$, includes not only the two squeezing forces, but also the weight. Thus, $f_{sqz}(t)$ can be calculated by subtracting the effect of the weight along $l(t)$ from $f_{r\downarrow sqz}(t)$:

$$f_{sqz}(t) = f_{r\downarrow sqz}(t) - f_{w\downarrow sqz}(t), \tag{10.12}$$

where $f_{w\downarrow sqz}(t)$ can be derived based on the third observation such that

$$f_{w\downarrow sqz}(t) = \left|\left(\mathbf{f}_{r,1}(t) + \mathbf{f}_{r,1}(t)\right)\cdot\mathbf{u}_l(t)\right|. \tag{10.13}$$

Then, the squeezing force at each contact point can be derived based on the first observation:

$$f_{sqz,1}(t) = f_{sqz,2}(t) = 0.5 f_{sqz}(t). \tag{10.14}$$

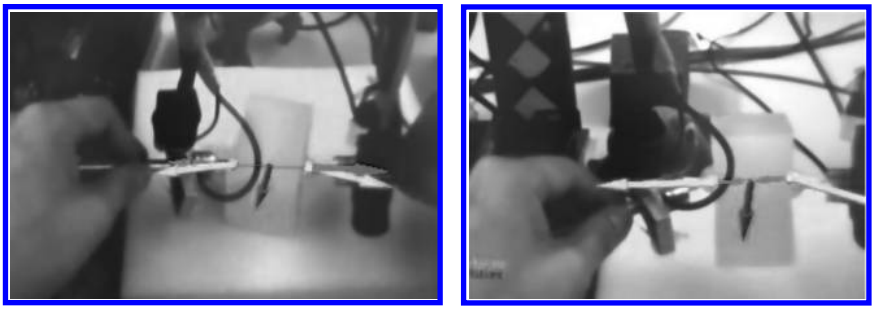

FIGURE 10.7 Example snapshot of visuo-haptic augmentation. Reaction force (dark gray arrow), weight (gray arrow), and haptic device force (light gray arrow) are depicted. Examples with increased stiffness (virtual forces oppose squeezing) and decreased stiffness (virtual forces assist squeezing) are shown on left and right, respectively.

Steps for the estimation of the displacement $x_*(t)$ in (10.11) are as follows. Let the distance between the two initial contact points on the non-deformed surface ($\mathbf{p}_{c,1}(t)$ and $\mathbf{p}_{c,2}(t)$ in Figure 10.6) be d_0. It is constant over time due to the no-slip assumption. Assuming homogeneity, $x_1(t)$ is equal to $x_2(t)$, and the displacements can be derived by

$$x_1(t) = x_2(t) = 0.5\left(d_0 - d(t)\right), \tag{10.15}$$

where $d(t)$ is $\left|\overline{\mathbf{p}_1(t)\mathbf{p}_2(t)}\right|$. All the unknown variables are now estimated and the final virtual force can be calculated using (10.11).

In Jeon and Harders (2012), we also evaluated the system performance through simulations and a psychophysical experiment. Overall, the evaluation indicated that our system can provide physically and perceptually sound stiffness augmentation. In addition, the system has further been integrated with a visual AR framework (Harders et al. 2009). To our knowledge, this is among the first system that can augment both visual and haptic sensations. We used the visual system to display information related to haptic augmentation, such as the force vectors involved in the algorithm. Figure 10.7 shows exemplar snapshots.

10.5 APPLICATION: PALPATING VIRTUAL INCLUSION IN PHANTOM WITH TWO CONTACTS

This section introduces an example of the applications of our stiffness modulation framework, taken from Jeon and Harders (2014). We developed algorithms for rendering a stiffer inclusion in a physical tissue phantom during manipulations at more than one contact location. The basic concept is depicted in Figure 10.8. The goal of the system is to render forces that give an illusion of a harder inclusion in the mock-up.

In Figure 10.8, $\mathbf{f}_{R,*}(t)$ are the reaction forces from the real environment to which the system adds virtual force feedback $\mathbf{f}_{T,*}(t)$ stemming from the simulated tumor

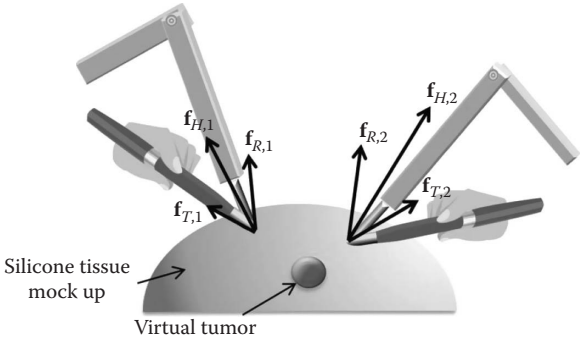

FIGURE 10.8 Overall configuration of rendering stiffer inclusion in real mock-up. (Reprinted from Jeon, S. and Harders, M., *IEEE Trans. Haptics*, 99, 1, 2014. With permission.)

with the consideration of the mutual effects between the contacts. The final combined forces $\mathbf{f}_{H,*}(t)$ enable a user to feel augmented sensations of the stiffer inclusion, given as

$$\mathbf{f}_{H,*}(t) = \mathbf{f}_{R,*}(t) + \mathbf{f}_{T,*}(t). \tag{10.16}$$

Here, estimating and simulating $\mathbf{f}_{T,*}(t)$ is the key for creating a sound illusion. The hardware setup we used is the same as the one shown in Figure 10.4.

A two-step, measurement-based approach is taken to model the dynamic behavior of the inclusion. First, a contact dynamics model representing the pure response of the inclusion is identified using the data captured during palpating a physical mock-up. Then, another dynamics model is constructed to capture the movement characteristics of the inclusion in response to external forces. Both models are then used in rendering to determine $\mathbf{f}_{T,*}(t)$ in real-time. The procedures are detailed in the following paragraphs.

The first preprocessing step is for identifying the overall contact force resulting purely from an inclusion (*inclusion-only* case) as a function of the distance between the inclusion and the contact point. Our approach is to extract the difference between the responses of a sample with a stiffer inclusion (*inclusion-embedded*) and a sample without it (*no-inclusion*). To this end, we first identify the Hunt–Crossley model using the no-inclusion model. We use the same identification procedure described in Section 10.4.2. This model is denoted by $f = H_{NT}(x,\dot{x})$. Then, we obtain the data from the inclusion-embedded sample by manually poking along a line from $\mathbf{p}_{Ts}$ to $\mathbf{p}_{T0}$ (see Figure 10.9 for the involved quantities). This time, we also record the position changes of $\mathbf{p}_T$ using a position tracking system (TrackIR; NaturalPoint, Inc.). This gives us the state vector when palpating the tumor-embedded model $(x_{TE}, \dot{x}_{TE}, f_{TE}, \mathbf{p}_T, \mathbf{p}_H)$.

As depicted in Figure 10.8, the force $f_{TE}(t)$ can be decomposed into $\mathbf{f}_R(t)$ and $\mathbf{f}_T(t)$. Since $f = H_{NT}(x,\dot{x})$ represents the magnitude of $\mathbf{f}_R(t)$, the magnitude of $\mathbf{f}_T(t)$ can be obtained by passing all data pairs $(x_{TE}, \dot{x}_{TE})$ to $H_{NT}(x,\dot{x})$ and by computing differences using

$$f_T\left(x_{TE}, \dot{x}_{TE}\right) = f_{TE} - H_{NT}\left(x_{TE}, \dot{x}_{TE}\right). \tag{10.17}$$

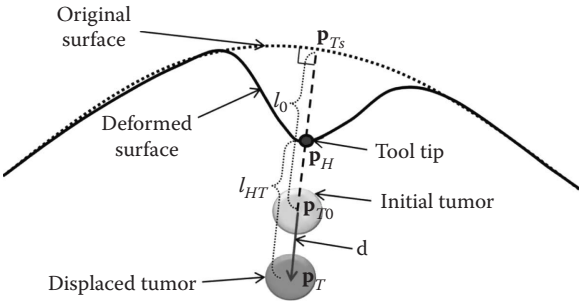

FIGURE 10.9 Variables for inclusion model identification. (Reprinted from Jeon, S. and Harders, M., *IEEE Trans. Haptics*, 99, 1, 2014. With permission.)

$f_T(t)$ can be expressed as a function of the distance between the inclusion and the tool tip. Let the distance from $\mathbf{p}_H(t)$ to $\mathbf{p}_T(t)$ be $l_{HT}(t)$, and the initial distance from $\mathbf{p}_{Ts}$ to $\mathbf{p}_{T0}$ be l_0. Then, the difference, $l(t) = l_0 - l_{HT}(t)$, becomes a relative displacement toward the inclusion. By using the data triples $(l, \dot{l}, f_T)$, a new response model with respect to $l(t)$ can be derived, which is denoted as $H_T(l, \dot{l})$. This represents the inclusion-only force response at the single contact point $\mathbf{p}_{Ts}$, poking into the direction of $\mathbf{p}_T$.

In the second step, the inclusion movement in response to external forces is characterized. Nonlinear changes of $\mathbf{d}(t)$ with respect to an external force $\mathbf{f}_T(t)$ can be approximated using again the Hunt–Crossley model. After determining $\mathbf{d}(t)$ using a position tracker and $\mathbf{f}_T(t)$ using our rendering algorithm described in the next subsection, vector triples $(\mathbf{d}, \dot{\mathbf{d}}, \mathbf{f}_T)$ are employed to identify three Hunt–Crossley models for the three Cartesian directions, denoted by $G_x(d_x, \dot{d}_x)$, $G_y(d_y, \dot{d}_y)$, and $G_z(d_z, \dot{d}_z)$.

10.5.1 Rendering Algorithm

Rendering begins with making a contact with the no-inclusion model. Forces from multiple contacts deform the model as shown in Figure 10.10 and displace the contact point from $\mathbf{p}_{Hs,*}$ to $\mathbf{p}_{H,*}(t)$ and the inclusion from $\mathbf{p}_{T0}$ to $\mathbf{p}_T(t)$. The force causing this movement is the same as the inclusion response at the user's hand $\mathbf{f}_{T,*}(t)$ in (10.15). Therefore, the direction of $\mathbf{f}_{T,*}(t)$ is from the inclusion position to the tool tip, such that

$$\mathbf{f}_{T,*}(t) = f_{T,*}(t) \frac{\mathbf{p}_{H,*}(t) - \mathbf{p}_T(t)}{|\mathbf{p}_{H,*}(t) - \mathbf{p}_T(t)|}. \tag{10.18}$$

Equation 10.18 indicates that the unknown values, $f_{T,*}(t)$ and $\mathbf{p}_T(t)$, should be approximated during the rendering.

$f_{T,*}(t)$ is derived based on H_T. To this end, we first scale the current indentation distance to match those during the recording:

$$l_*(t) = (l_{0,*} - l_{HT,*}(t)) \frac{l_0}{l_{0,*}}. \tag{10.19}$$

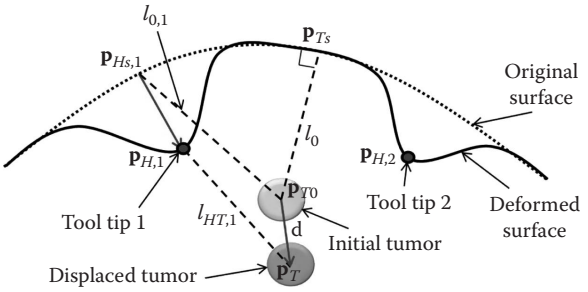

FIGURE 10.10 Variables for inclusion augmentation rendering. (Reprinted from Jeon, S. and Harders, M., *IEEE Trans. Haptics*, 99, 1, 2014. With permission.)

Then, we can obtain a linearly-normalized indentation length along $\overline{\mathbf{p}_{H,*}\mathbf{p}_T}$ with respect to the reference deformation. Finally, $f_{T,*}(t)$ is approximated by $f_{T,*}(t) = H_T(l_*(t), \dot{l}_*(t))$.

We take a similar approach for the update of $\mathbf{d}(t)$, and then eventually $\mathbf{p}_T(t)$. Taking the inverse of $G_{x,y,z}$ allows us to approximate $\mathbf{d}(t)$ by

$$d_i(t) = \left\{ \frac{\sum_{*=1}^{n} f_{T,*,i}(t)}{k + b\,d(t)} \right\}^{1/m} \qquad i = x, y, z, \tag{10.20}$$

where

n is the number of contact points

m is the exponential parameter in the Hunt–Crossley model

Finally, $\mathbf{f}_{T,*}(t)$ is determined using (10.18), which is directly sent to the haptic AR interface.

In Jeon and Harders (2014), we compared the simulation results of our algorithm with actual measurement data recorded from eight different real mock-ups via various interaction methods. Overall, inclusion movements and the mutual effects between contacts are captured and simulated with reasonable accuracy; the force simulation errors were less than the force perception thresholds in most cases.

10.6 FRICTION MODULATION

Our next target was the modulation of surface friction (Jeon et al. 2011). Here, we introduce simple and effective algorithms for estimating and altering inherent friction between a tool tip and a surface to desired friction. We also use the same hardware setup for friction modulation.

The specific goal of this work is to alter real friction force $f_{real}(t)$ such that a user perceives a modulated friction force $f_{targ}(t)$ that mimics the response of a surface made of a different desired target material when the user strokes the real surface

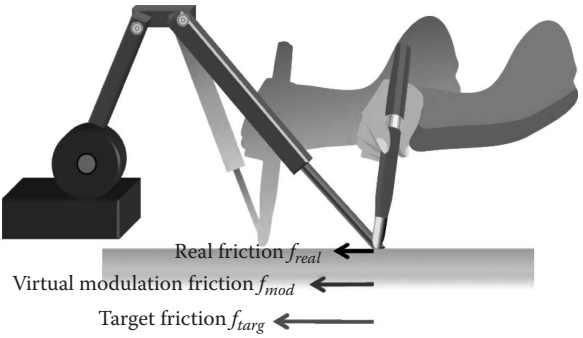

FIGURE 10.11 Variables for friction modulation. (Reprinted from Jeon, S. et al., Extensions to haptic augmented reality: Modulating friction and weight, in *Proceedings of the IEEE World Haptics Conference (WHC)*, 2011, pp. 227–232. With permission.)

with a tool. As illustrated in Figure 10.11, this is done by adding a modulation friction force $f_{mod}(t)$ to the real friction force:

$$f_{mod}(t) = f_{targ}(t) - f_{real}(t). \tag{10.21}$$

Thus, the task reduces to: (1) simulation of the desired friction response $f_{targ}(t)$ and (2) measurement of the real friction force $f_{real}(t)$.

For the simulation of the desired friction force $f_{targ}(t)$ during rendering, we identify the modified Dahl model describing the friction of a target surface. For the Dahl model parameter identification, a user repeatedly strokes the target surface with the probe tip attached to the PHANToM. The identification procedure is the same as that given in Section 10.4.2. The model is then used to calculate $f_{targ}(t)$ using the tool tip position and velocity and the normal contact force during augmented rendering.

$f_{real}(t)$ can be easily derived from force sensor readings after a noise reduction process. Given the real friction and the target friction, the appropriate modulation force that needs to be rendered by the device is finally computed using (10.20). The modulation force is sent to the haptic interface for force control.

We tested the accuracy of our friction identification and modulation algorithms with four distinctive surfaces (Jeon et al. 2011). The results showed that regardless of the base surface, the friction was modulated to a target surface without perceptually significant errors.

10.7 OPEN RESEARCH TOPICS

In spite of our and other groups' endeavor for haptic AR, this field is still young and immature, awaiting persistent research on many intriguing and challenging topics. For instance, our work regarding stiffness modulation has focused on *homogeneous* soft real objects, meaning that the material characteristics of the objects are identical regardless of contact point. However, most natural deformable objects exhibit inhomogeneity. Such objects show much more complicated deformation and friction

behaviors, and approaches that are based on more in-depth contact mechanics are necessary for appropriate modeling and augmentation. This has been one direction of our research, with an initial result that allows the user to model the shape of a soft object using a haptic interface without the need for other devices (Yim and Choi 2012).

Our work has used a handheld tool for the exploration of real objects. This must be extended to those which allow for the use of bare hands, or at least very similar cases such as thin thimbles enclosing fingertips. Such extension will enlarge the application area of haptic AR by the great extent, for example, palpation training on a real phantom that includes virtual organs and lumps. To this end, we have begun to examine the feasibility of sensing not only contact force but also contact pressure in a compact device and its utility for haptic AR (Kim et al. 2014).

Another important topic is that for multi-finger interaction. This functionality requires very complicated haptic interfaces that provide multiple, independent forces with a very large degrees of freedom (see Barbagli et al. 2005), as well as very sophisticated deformable body rendering algorithms that take into account the interplay between multiple contacts. Research effort on this topic is still ongoing even for haptic VR.

Regarding material properties, we need methods to augment friction, texture, and temperature. Friction is expected to be relatively easier in both modeling and rendering for haptic AR, as long as deformation is properly handled. Temperature modulation is likely to be more challenging, especially due to the difficulty of integrating a temperature display to the fingertip that touches real objects. This functionality can greatly improve the realism of AR applications.

The last critical topic we wish to mention is texture. Texture is one of the most salient material properties and determines the identifying tactual characteristics of an object (Katz 1925). As such, a great amount of research has been devoted to haptic perception and rendering of surface texture. Texture is also one of the most complex issues because of the multiple perceptual dimensions involved in texture perception; all of surface microgeometry and material's elasticity, viscosity, and friction play an important role (Hollins et al. 1993, 2000). See Choi and Tan (2004a,b, 2005, 2007) for a review of texture perception relevant to haptic rendering, Campion and Hayward (2007) for passive rendering of virtual textures, and Fritz and Barner (1996), Guruswamy et al. (2011), Lang and Andrews (2011), and Romano and Kuchenbecker (2011) for various models. All of these studies pertained to haptic VR rendering. Among these, the work of Kuchenbecker and her colleagues has the best feasibility for application to haptic AR; they have developed a high-quality texture rendering system that overlays artificial vibrations on a touchscreen to deliver the textures of real samples (Romano and Kuchenbecker 2011) and an open database of textures (Culbertson et al. 2014). This research can be a cornerstone for the modeling and augmentation of real textures.

10.8 CONCLUSIONS

This chapter overviewed the emerging AR paradigm for the sense of touch. We first outlined the conceptual, functional, and technical aspects of this new paradigm with three taxonomies and thorough review of existing literature. Then, we moved to

recent attempts for realizing haptic AR, where hardware and algorithms for augmenting the stiffness and friction of a real object were detailed. These frameworks are applied to medical training of palpation, where stiffer virtual inclusions are rendered in a real tissue mock-up. Lastly, we elucidate several challenges and future research topics in this research area. We hope that our endeavor introduced in this chapter will pave the way to more diverse and mature researches in the exciting field of haptic AR.

REFERENCES

Abbott, J., P. Marayong, and A. Okamura. 2007. Haptic virtual fixtures for robot-assisted manipulation. In *Robotics Research*, eds. S. Thrun, R. Brooks, and H. Durrant-Whyte, pp. 49–64. Springer-Verlag: Berlin, Germany.

Abbott, J. and A. Okamura. 2003. Virtual fixture architectures for telemanipulation. *Proceedings of the IEEE International Conference on Robotics and Automation*, pp. 2798–2805. Taipei, Taiwan.

Adcock, M., M. Hutchins, and C. Gunn. 2003. Augmented reality haptics: Using ARToolKit for display of haptic applications. *Proceedings of Augmented Reality Toolkit Workshop*, pp. 1–2. Tokyo, Japan.

Azuma, R., Y. Baillot, R. Behringer, S. Feiner, S. Julier, and B. MacIntyre. 2001. Recent advances in augmented reality. *IEEE Computer Graphics & Applications* 21 (6):34–47.

Barbagli, F., D. Prattichizzo, and K. Salisbury. 2005. A multirate approach to haptic interaction with deformable objects single and multipoint contacts. *International Journal of Robotics Research* 24 (9):703–716.

Bayart, B., J. Y. Didier, and A. Kheddar. 2008. Force feedback virtual painting on real objects: A paradigm of augmented reality haptics. *Lecture Notes in Computer Science (EuroHaptics 2008)* 5024:776–785.

Bayart, B., A. Drif, A. Kheddar, and J.-Y. Didier. 2007. Visuo-haptic blending applied to a tele-touch-diagnosis application. *Lecture Notes on Computer Science (Virtual Reality, HCII 2007)* 4563: 617–626.

Bayart, B. and A. Kheddar. 2006. Haptic augmented reality taxonomy: Haptic enhancing and enhanced haptics. *Proceedings of EuroHaptics*, 641–644. Paris, France.

Bennett, E. and B. Stevens. 2006. The effect that the visual and haptic problems associated with touching a projection augmented model have on object-presence. *Presence: Teleoperators and Virtual Environments* 15 (4):419–437.

Bianchi, G., C. Jung, B. Knoerlein, G. Szekely, and M. Harders. 2006a. High-fidelity visuo-haptic interaction with virtual objects in multi-modal AR systems. *Proceedings of the IEEE and ACM International Symposium on Mixed and Augmented Reality*, pp. 187–196. Santa Barbara, USA.

Bianchi, G., B. Knoerlein, G. Szekely, and M. Harders. 2006b. High precision augmented reality haptics. *Proceedings of EuroHaptics*, pp. 169–168. Paris, France.

Billinghurst, M., H. Kato, and I. Poupyrev. 2001. The MagicBook—Moving seamlessly between reality and virtuality. *IEEE Computer Graphics & Applications* 21 (3):6–8.

Borst, C. W. and R. A. Volz. 2005. Evaluation of a haptic mixed reality system for interactions with a virtual control panel. *Presence: Teleoperators and Virtual Environments* 14 (6):677–696.

Bose, B., A. K. Kalra, S. Thukral, A. Sood, S. K. Guha, and S. Anand. 1992. Tremor compensation for robotics assisted microsurgery. *Engineering in Medicine and Biology Society, 1992, 14th Annual International Conference of the IEEE*, October 29, 1992–November 1 1992, pp. 1067–1068. Paris, France.

Brewster, S. and L. M. Brown. 2004. Tactons: Structured tactile messages for non-visual information display. *Proceedings of the Australasian User Interface Conference*, pp. 15–23. Dunedin, New Zealand.

Brown, L. M. and T. Kaaresoja. 2006. Feel who's talking: Using tactons for mobile phone alerts. *Proceeding of the Annual SIGCHI Conference on Human Factors in Computing Systems*, pp. 604–609. Montréal, Canada.

Campion, G. and V. Hayward. 2007. On the synthesis of haptic textures. *IEEE Transactions on Robotics* 24 (3):527–536.

Choi, S. and H. Z. Tan. 2004a. Perceived instability of virtual haptic texture. I. Experimental studies. *Presence: Teleoperators and Virtual Environment* 13 (4):395–415.

Choi, S. and H. Z. Tan. 2004b. Toward realistic haptic rendering of surface textures. *IEEE Computer Graphics & Applications (Special Issue on Haptic Rendering—Beyond Visual Computing)* 24 (2):40–47.

Choi, S. and H. Z. Tan. 2005. Perceived instability of haptic virtual texture. II. Effects of collision detection algorithm. *Presence: Teleoperators and Virtual Environments* 14 (4):463–481.

Choi, S. and H. Z. Tan. 2007. Perceived instability of virtual haptic texture. III. Effect of update rate. *Presence: Teleoperators and Virtual Environments* 16 (3):263–278.

Chun, J., I. Lee, G. Park, J. Seo, S. Choi, and S. H. Han. 2013. Efficacy of haptic blind spot warnings applied through a steering wheel or a seatbelt. *Transportation Research Part F: Traffic Psychology and Behaviour* 21:231–241.

Culbertson, H., J. J. L. Delgado, and K. J. Kuchenbecker. 2014. One hundred data-driven haptic texture models and open-source methods for rendering on 3D objects. *Proceedings of the IEEE Haptics Symposium*, pp. 319–325. Houston, TX.

Feng, Z., H. B. L. Duh, and M. Billinghurst. 2008. Trends in augmented reality tracking, interaction and display: A review of ten years of ISMAR. *Proceedings of the IEEE/ACM International Symposium of Mixed and Augmented Reality*, pp. 193–202. Cambridge, UK.

Frey, M., J. Hoogen, R. Burgkart, and R. Riener. 2006. Physical interaction with a virtual knee joint—The 9 DOF haptic display of the Munich knee joint simulator. *Presence: Teleoperators and Virtual Environment* 15 (5):570–587.

Fritz, J. P. and K. E. Barner. 1996. Stochastic models for haptic texture. *Proceedings of SPIE's International Symposium on Intelligent Systems and Advanced Manufacturing—Telemanipulator and Telepresence Technologies III*, pp. 34–44. Boston, MA.

Fukumoto, M. and T. Sugimura. 2001. Active click: Tactile feedback for touch panels. *Proceedings of the SIGCHI Conference on Human Factors in Computing Systems*, pp. 121–122. Seattle, WA.

Gerling, G. J. and G. W. Thomas. 2005. Augmented, pulsating tactile feedback facilitates simulator training of clinical breast examinations. *Human Factors* 47 (3):670–681.

Gopal, P., S. Kumar, S. Bachhal, and A. Kumar. 2013. Tremor acquisition and reduction for robotic surgical applications. *Proceedings of International Conference on Advanced Electronic Systems*, pp. 310–312. Pilani, India.

Grosshauser, T. and T. Hermann. 2009. Augmented haptics—An interactive feedback system for musicians. *Lecture Notes in Computer Science (HAID 2012)* 5763:100–108.

Guruswamy, V. L., J. Lang, and W.-S. Lee. 2011. IIR filter models of haptic vibration textures. *IEEE Transactions on Instrumentation and Measurement* 60 (1):93–103.

Ha, T., Y. Chang, and W. Woo. 2007. Usability test of immersion for augmented reality based product design. *Lecture Notes in Computer Science (Edutainment 2007)* 4469:152–161.

Ha, T., Y. Kim, J. Ryu, and W. Woo. 2006. Enhancing immersiveness in AR-based product design. *Lecture Notes in Computer Science (ICAT 2006)* 4282:207–216.

Hachisu, T., M. Sato, S. Fukushima, and H. Kajimoto. 2012. Augmentation of material property by modulating vibration resulting from tapping. *Lecture Notes in Computer Science (EuroHaptics 2012)* 7282:173–180.

Haddadi, A. and K. Hashtrudi-Zaad. 2008. A new method for online parameter estimation of hunt-crossley environment dynamic models. *Proceedings of the IEEE International Conference on Intelligent Robots and Systems*, pp. 981–986. Nice, France.

Harders, M., G. Bianchi, B. Knoerlein, and G. Szekely. 2009. Calibration, registration, and synchronization for high precision augmented reality haptics. *IEEE Transactions on Visualization and Computer Graphics* 15 (1):138–149.

Hoever, R., G. Kosa, G. Szekely, and M. Harders. 2009. Data-driven haptic rendering-from viscous fluids to visco-elastic solids. *IEEE Transactions on Haptics* 2:15–27.

Hollins, M., S. J. Bensmäi, K. Karlof, and F. Young. 2000. Individual differences in perceptual space for tactile textures: Evidence from multidimensional scaling. *Perception & Psychophysics* 62 (8):1534–1544.

Hollins, M., R. Faldowski, R. Rao, and F. Young. 1993. Perceptual dimensions of tactile surfaced texture: A multidimensional scaling analysis. *Perception & Psychophysics* 54:697–705.

Hugues, O., P. Fuchs, and O. Nannipieri. 2011. New augmented reality taxonomy: Technologies and features of augmented environment. In *Handbook of Augmented Reality*, ed. B. Furht, pp. 47–63. Springer-Verlag: Berlin, Germany.

Hunt, K. and F. Crossley. 1975. Coefficient of restitution interpreted as damping in vibroimpact. *ASME Journal of Applied Mechanics* 42:440–445.

Iwata, H., H. Yano, F. Nakaizumi, and R. Kawamura. 2001. Project FEELEX: Adding haptic surface to graphics. *Proceedings of ACM SIGGRAPH*, pp. 469–476. Los Angeles, CA.

Jeon, S. and S. Choi. 2008. Modulating real object stiffness for haptic augmented reality. *Lecture Notes on Computer Science (EuroHaptics 2008)* 5024:609–618.

Jeon, S. and S. Choi. 2009. Haptic augmented reality: Taxonomy and an example of stiffness modulation. *Presence: Teleoperators and Virtual Environments* 18 (5):387–408.

Jeon, S. and S. Choi. 2010. Stiffness modulation for haptic augmented reality: Extension to 3D interaction. *Proceedings of the Haptics Symposium*, pp. 273–280. Waltham, MA.

Jeon, S. and S. Choi. 2011. Real stiffness augmentation for haptic augmented reality. *Presence: Teleoperators and Virtual Environments* 20 (4):337–370.

Jeon, S. and M. Harders. 2012. Extending haptic augmented reality: Modulating stiffness during two-point squeezing. *Proceedings of the Haptics Symposium*, pp. 141–146. Vancouver, Canada.

Jeon, S. and M. Harders. 2014. Haptic tumor augmentation: Exploring multi-point interaction. *IEEE Transactions on Haptics* 99 (Preprints):1–1.

Jeon, S., M. Harders, and S. Choi. 2012. Rendering virtual tumors in real tissue mock-ups using haptic augmented reality. *IEEE Transactions on Haptics* 5 (1):77–84.

Jeon, S., J.-C. Metzger, S. Choi, and M. Harders. 2011. Extensions to haptic augmented reality: Modulating friction and weight. *Proceedings of the IEEE World Haptics Conference (WHC)*, pp. 227–232. Istanbul, Turkey.

Johnson, A., D. Sandin, G. Dawe, T. DeFanti, D. Pape, Z. Qiu, and D. P. S. Thongrong. 2000. Developing the PARIS: Using the CAVE to prototype a new VR display. *Proceedings of the ACM Symposium on Immersive Projection Technology*.

Kajimoto, H., N. Kawakami, S. Tachi, and M. Inami. 2004. SmartTouch: Electric skin to touch the untouchable. *IEEE Computer Graphics & Applications* 24 (1):36–43.

Katz, D. 1925. *The World of Touch*. Hillsdale, NJ: Lawrence Erlbaum Associates.

Kim, H., S. Choi, and W. K. Chung. 2014. Contact force decomposition using tactile information for haptic augmented reality. *Proceedings of the IEEE/RSJ International Conference on Robots and Systems*, pp. 1242–1247. Chicago, IL.

Kim, S., J. Cha, J. Kim, J. Ryu, S. Eom, N. P. Mahalik, and B. Ahn. 2006. A novel test-bed for immersive and interactive broadcasting production using augmented reality and haptics. *IEICE Transactions on Information and Systems* E89-D (1):106–110.

Kim, S.-Y. and J. C. Kim. 2012. Vibrotactile rendering for a traveling vibrotactile wave based on a haptic processor. *IEEE Transactions on Haptics* 5 (1):14–20.

Kurita, Y., A. Ikeda, T. Tamaki, T. Ogasawara, and K. Nagata. 2009. Haptic augmented reality interface using the real force response of an object. *Proceedings of the ACM Virtual Reality Software and Technology*, pp. 83–86. Kyoto, Japan.

Kyung, K.-U. and J.-Y. Lee. 2009. Ubi-Pen: A haptic interface with texture and vibrotactile display. *IEEE Computer Graphics and Applications* 29 (1):24–32.

Lang, J. and S. Andrews. 2011. Measurement-based modeling of contact forces and textures for haptic rendering. *IEEE Transactions on Visualization and Computer Graphics* 17 (3):380–391.

Lee, H., W. Kim, J. Han, and C. Han. 2012a. The technical trend of the exoskeleton robot system for human power assistance. *International Journal of Precision Engineering and Manufacturing* 13 (8):1491–1497.

Lee, I. and S. Choi. 2014. Vibrotactile guidance for drumming learning: Method and perceptual assessment. *Proceedings of the IEEE Haptics Symposium*, pp. 147–152. Houston, TX.

Lee, I., K. Hong, and S. Choi. 2012. Guidance methods for bimanual timing tasks. *Proceedings of IEEE Haptics Symposium*, pp. 297–300. Vancouver, Canada.

Li, M., M. Ishii, and R. H. Taylor. 2007. Spatial motion constraints using virtual fixtures generated by anatomy. *IEEE Transactions on Robotics* 23 (1):4–19.

Luciano, C., P. Banerjee, L. Florea, and G. Dawe. 2005. Design of the ImmersiveTouch™: A high-performance haptic augmented virtual reality system. *Proceedings of International Conference on Human-Computer Interaction*. Las Vegas, NV.

Mahvash, M. and A. M. Okamura. 2006. Friction compensation for a force-feedback telerobotic system. *Proceedings of the IEEE International Conference on Robotics and Automation*, pp. 3268–3273. Orlando, FL.

Milgram, P. and H. Colquhoun, Jr. 1999. A taxonomy of real and virtual world display integration. In *Mixed Reality—Merging Real and Virtual Worlds*, ed. by Y. O. A. H. Tamura, pp. 1–16. Springer-Verlag: Berlin, Germany.

Minamizawa, K., H. Kajimoto, N. Kawakami, and S. Tachi. 2007. Wearable haptic display to present gravity sensation. *Proceedings of the World Haptics Conference*, pp. 133–138. Tsukuba, Japan

Mitchell, B., J. Koo, M. Iordachita, P. Kazanzides, A. Kapoor, J. Handa, G. Hager, and R. Taylor. 2007. Development and application of a new steady-hand manipulator for retinal surgery. *Proceedings of the IEEE International Conference on Robotics and Automation*, pp. 623–629. Rome, Italy.

Nojima, T., D. Sekiguchi, M. Inami, and S. Tachi. 2002. The SmartTool: A system for augmented reality of haptics. *Proceedings of the IEEE Virtual Reality Conference*, pp. 67–72. Orlando, FL.

Ochiai, Y., T. Hoshi, J. Rekimoto, and M. Takasaki. 2014. Diminished haptics: Towards digital transformation of real world textures. *Lecture Notes on Computer Science (Eurohaptics 2014, Part I)* LNCS 8618: pp. 409–417.

Okamura, A. M., M. R. Cutkosky, and J. T. Dennerlein. 2001. Reality-based models for vibration feedback in virtual environments. *IEEE/ASME Transactions on Mechatronics* 6 (3):245–252.

Ott, R., D. Thalmann, and F. Vexo. 2007. Haptic feedback in mixed-reality environment. *The Visual Computer: International Journal of Computer Graphics* 23 (9):843–849.

Pai, D. K., K. van den Doel, D. L. James, J. Lang, J. E. Lloyd, J. L. Richmond, and S. H. Yau. 2001. Scanning physical interaction behavior of 3D objects. *Proceedings of the Annual Conference on ACM Computer Graphics and Interactive Techniques*, pp. 87–96. Los Angeles, CA.

Park, G., S. Choi, K. Hwang, S. Kim, J. Sa, and M. Joung. 2011. Tactile effect design and evaluation for virtual buttons on a mobile device Touchscreen. *Proceedings of the International Conference on Human-Computer Interaction with Mobile Devices and Services (MobileHCI)*, pp. 11–20. Stockholm, Sweden.

Parkes, R., N. N. Forrest, and S. Baillie. 2009. A mixed reality simulator for feline abdominal palpation training in veterinary medicine. *Studies in Health Technology and Informatics* 142:244–246.

Powell, D. and M. K. O'Malley. 2011. Efficacy of shared-control guidance paradigms for robot-mediated training. *Proceedings of the IEEE World Haptics Conference*, pp. 427–432. Istanbul, Turkey.

Reachin Technology. Reachin Display. http://www.reachin.se/. Accessed March 4, 2015.

Romano, J. M. and K. J. Kuchenbecker. 2011. Creating realistic virtual textures from contact acceleration data. *IEEE Transactions on Haptics* 5 (2):109–119.

Rosenberg, L. B. 1993. Virtual fixtures: Perceptual tools for telerobotic manipulation. *Proceedings of the IEEE Virtual Reality Annual International Symposium*, pp. 76–82.

Rovers, L. and H. van Essen. 2004. Design and evaluation of hapticons for enriched instant messaging. *Proceedings of Eurohaptics*, pp. 498–503. Munich, Germany.

Sandor, C., S. Uchiyama, and H. Yamamoto. 2007. Visuo-haptic systems: Half-mirrors considered harmful. *Proceedings of the World Haptics Conference*, pp. 292–297. Tsukuba, Japan.

Scharver, C., R. Evenhouse, A. Johnson, and J. Leigh. 2004. Designing cranial implants in a haptic augmented reality environment. *Communications of the ACM* 47 (8):32–38.

SenseGraphics. 3D-IW. http://www.sensegraphics.se/. Accessed on March 4, 2015.

SoIanki, M. and V. Raja. 2010. Haptic based augmented reality simulator for training clinical breast examination. *Proceedings of the IEEE Conference on Biomedical Engineering and Sciences*, pp. 265–269. Kuala Lumpur, Malaysia.

Spence, C. and C. Ho. 2008. Tactile and multisensory spatial warning signals for drivers. *IEEE Transactions on Haptics* 1 (2):121–129.

Sreng, J., A. Lecuyer, and C. Andriot. 2008. Using vibration patterns to provide impact position information in haptic manipulation of virtual objects. *Lecture Notes on Computer Science (EuroHaptics 2008)* 5024:589–598.

Ternes, D. and K. E. MacLean. 2008. Designing large sets of haptic icons with rhythm. *Lecture Notes on Computer Science (EuroHaptics 2008)* 5024:199–208.

Vallino, J. R. and C. M. Brown. 1999. Haptics in augmented reality. *Proceedings of the IEEE International Conference on Multimedia Computing and Systems*, pp. 195–200. Florence, Italy.

Yang, C., J. Zhang, I. Chen, Y. Dong, and Y. Zhang. 2008. A review of exoskeleton-type systems and their key technologies. *Proceedings of the Institution of Mechanical Engineers, Part C: Journal of Mechanical Engineering Science* 222 (8):1599–1612.

Yao, H.-Y., V. Hayward, and R. E. Ellis. 2004. A tactile magnification instrument for minimally invasive surgery. *Lecture Notes on Computer Science (MICCAI)* 3217:89–96.

Ye, G., J. Corso, G. Hager, and A. Okamura. 2003. VisHap: Augmented reality combining haptics and vision. *Proceedings of the IEEE International Conference on Systems, Man and Cybernetics*, pp. 3425–3431. Washington, D.C.

Yim, S. and S. Choi. 2012. Shape modeling of soft real objects using force-feedback haptic interface. *Proceedings of the IEEE Haptics Symposium*, pp. 479–484. Vancouver, Canada.

Yokokohji, Y., R. L. Hollis, and T. Kanade. 1999. WYSIWYF display: A visual/haptic interface to virtual environment. *Presence: Teleoperators and Virtual Environments* 8 (4):412–434.

Zoran, A. and J. A. Paradiso. 2012. The FreeD—A handheld digital milling device for craft and fabrication. *Proceedings of the ACM Symposium on User Interface Software and Technology*, pp. 3–4. Toronto, Canada.